Annals of Nuclear Medicine
https://doi.org/10.1007/s12149-024-01947-z

SHORT COMMUNICATION

DOCK–PET: database of CNS kinetic parameters in the healthy human brain for existing PET tracers

Itsuki Miyajima[1] · Ayano Yoshikawa[1] · Kyosei Sahashi[1] · Chie Seki[2] · Yuji Nagai[2] · Hiroshi Watabe[3] · Miho Shidahara[1]

Received: 27 October 2023 / Accepted: 24 April 2024

Abstract

Purpose Information about developed positron emission tomography (PET) tracers and obtained clinical PET images is publicly available in a database. However, findings regarding the kinetic parameters of PET tracers are yet to be summarized. Therefore, in this study, we created an open-access database of central nervous system (CNS) kinetic parameters in the healthy human brain for existing PET tracers (DOCK–PET).

Methods Our database includes information on the kinetic parameters and compounds of existing CNS–PET tracers. The kinetic parameter dataset comprises the analysis methods, V_T, BP_{ND}, K parameters, relevant literature, and study details. The list of PET tracers and kinetic parameter information was compiled through keyword-based searches of PubMed and the Molecular Imaging and Contrast Agent Database (MICAD). The kinetic parameters obtained, including V_T, $BP_{ND,}$ and K parameters, were reorganized based on the defined brain anatomical regions. All data were rigorously double-checked before being summarized in Microsoft Excel and JavaScript Object Notation (JSON) formats.

Results Of the 247 PET tracers identified through searches using the PubMed and MICAD websites, the kinetic parameters of 120 PET tracers were available. Among the 120 PET tracers, compound structures with chemical and physical properties were obtained from the PubChem website or the ChemDraw software. Furthermore, the affinity information of the 104 PET tracers was gathered from PubChem or extensive literature surveys of the 120 PET tracers.

Conclusions We developed a comprehensive open-access database, DOCK–PET, that includes both kinetic parameters of healthy humans and compound information for existing CNS–PET tracers.

Keywords CNS–PET · Database · Kinetic parameters · Healthy human brain

Introduction

PET tracer

Positron emission tomography (PET) enables visualization of biological functions in vivo and is used for clinical diagnosis and basic research. A PET tracer is a radiopharmaceutical labeled with the radioisotope of a positron emitter, and its pharmacokinetics are crucial for functional imaging. Half a century has passed since the first clinical PET study was reported in the 1970s [1, 2]. Numerous PET tracers have been developed, and most have been registered in the open chemistry database PubChem (https://pubchem.ncbi.nlm.nih.gov), which is the most extensive collection of freely accessible compounds.

Database of drugs and collective intelligence

Several open-access databases have been established, for the development of therapeutic drugs, including approved drugs (https://go.drugbank.com), clinical trials (https://clinicaltrials.gov), and adverse event reporting systems (https://open.fda.gov/data/faers). These databases contain information on existing drugs that have progressed to clinical use. In the

✉ Miho Shidahara
miho.shidahara.c2@tohoku.ac.jp

[1] Department of Quantum Science and Energy Engineering, Graduate School of Engineering, Tohoku University, Sendai, Japan

[2] Advanced Neuroimaging Center, Institute for Quantum Medical Science, National Institutes for Quantum Science and Technology, Chiba, Japan

[3] Division of Radiation Protection and Nuclear Safety, Research Center for Accelerator and Radioisotope Science, Tohoku University, Sendai, Japan

Published online: 30 May 2024

quest to discover and develop novel drugs, researchers not only rely on databases of existing drugs but also turn to other types of databases. One example is the Research Collaboratory for Structural Bioinformatics (RCSB) Protein Data Bank, which aids in predicting the properties of candidate drugs. These predictions cover factors, such as the likelihood of adverse events based on AC50 (the concentration that produces 50% activation) [3], ligand affinity determined by protein structure and ligand properties [4], and metabolite identification based on molecular structure [5]. Moreover, collaborative networks, such as the Japanese Drug Alliance Network, have been established through partnerships between PET academia and pharmaceutical companies, representing a form of collective intelligence [6]. The ongoing digital transformation (DX) process harnesses the power of extensive databases and collective intelligence to drive the discovery and development of therapeutic drugs.

Database of PET imaging and tracers

As PET is primarily an imaging modality, several imaging databases are available, such as the amyloid PET database provided by the Alzheimer's Disease Neuroimaging Initiative (ADNI, https://adni.loni.usc.edu), CNS–PET data accessible through Open Neuro (https://openneuro.org/search/modality/pet), and other proposed image repository systems [7].

The Brain Imaging Data Structure (BIDS) is a data format designed for the structured organization of neuroimaging and behavioral data [8]. More recently, PET–BIDS was introduced as an extension of the original BIDS format, encompassing PET images and associated text datasets, such as blood sampling results [9]. PET–BIDS focuses on the distribution of raw dynamic data with PET study information, not the kinetic analysis's outcome.

Regarding PET tracer databases, PubChem is a valuable resource containing compound structures, names, identifiers (including computed descriptors and synonyms), and chemical and physical properties such as molecular weight and biological assay data. Professor Iwata at Tohoku University compiled the Reference Book 2004 for PET Radiopharmaceuticals, which provides information on chemical structures and their references (https://www.cyric.tohoku.ac.jp/kakuyaku/public/preface2004.html). Furthermore, because PET tracers involve a radiosynthesis process distinct from that of treatment drugs, helpful databases on methods of radiosynthesis are available (https://www.nirs.qst.go.jp/research/division/mic/db2/index.html). McCluskey et al. summarized the state-of-the-art of PET radiopharmaceuticals for new imaging targets [10]. Although PET imaging data and information on existing PET tracers are available as open data sources, a comprehensive summary of kinetic parameters has not yet been compiled.

Database of pharmacokinetics of CNS–PET tracers

For diagnostic purposes, CNS–PET tracers are expected to exhibit favorable pharmacokinetics in the brain. Good pharmacokinetics can be defined by criteria such as (i) high blood–brain barrier permeability, (ii) strong affinity for the target molecule, (iii) minimal nonspecific binding or accumulation, and (iv) absence of radioactive metabolite entry into the brain, among other factors [11]. Kinetic parameters are critical indicators for evaluating the pharmacokinetics of PET tracers. In this study, we established a novel open-access database of CNS kinetic parameters in the healthy human brain for existing PET tracers named as DOCK–PET. These kinetic parameters were mathematically estimated using the observed PET time-activity curves in the brains of healthy subjects and pharmacokinetic models.

Materials and methods

Existing CNS–PET tracers

The imaging targets encompass a wide range of biological entities, including acetylcholinesterase, adenosine receptor, α2-adrenoceptor, amyloid-β deposits, aromatic l-amino acid decarboxylase, beta-secretase 1, benzodiazepine receptor, cannabinoid receptor 1 (CB1), dopamine system, fatty acid amide hydrolase, glucose metabolism, glycine transporter type-1, histamine receptor, histone deacetylases, metabotropic glutamine receptor, mitochondrial complex 1, monoamine oxidase, muscarinic acetylcholine receptor, nicotinic acetylcholine receptor, neurokinin 1 receptor, O-linked-β-N-acetyl-glucosamine hydrolase, opioid receptor, phosphodiesterase, serotonin system, synaptic vesicle protein 2A, translocator protein, and σ1 receptor.

Existing CNS–PET tracers that had undergone clinical studies were identified through searches of PubMed databases as of January 19, 2023, and on the Molecular Imaging and Contrast Agent Database (MICAD) as of May 10, 2023. In addition, a separate search for amyloid PET tracers was conducted using the PubMed database on August 10, 2023. For each imaging target, PET tracers were identified using a combination of relevant keywords (e.g., target name, human, CNS, and PET). The PubMed search strategy in Supplemental Table 1 yielded 138 PET tracers. Among these, regional kinetic parameters from healthy subjects have been documented for 87 PET tracers. The MICAD search identified 109 PET tracers, 26 of which overlapped with those found in PubMed, and

Table 1 The number of PET tracers for each imaging target

Imaging target	The number of PET tracers	Imaging target	The number of PET tracers
Acetylcholinesterase	2	Muscarinic acetylcholine receptor subtype M1	1
Adenosine A_1 receptor	2	Nicotinic acetylcholine receptor	1
Adenosine A_{2A} receptor	2	α_7-nicotinic acetylcholine receptor	1
α_2-Adrenoceptor	1	Neurokinin 1 receptor	2
Amyloid-β deposits	9	O-linked-β-N-acetyl-glucosamine hydrolase	1
Aromatic l – amino acid decarboxylase	1	Opioid receptor	2
Beta-secretase 1	1	μ-opioid receptor	1
Benzodiazepine receptor	4	κ-opioid receptor	4
Cannabinoid receptor 1 (CB1)	3	δ-opioid receptor	1
Dopamine transporter	6	Opioid receptor like-1 receptor	1
Dopamine D_1 receptor	1	Phosphodiesterase-2A	1
Dopamine D_2/D_3 receptor	9	Phosphodiesterase-4	1
Fatty acid amide hydrolase	1	Phosphodiesterase-7	1
Glucose metabolism	1	Phosphodiesterase-10A	5
Glycine transporter type-1	1	P2X7 purinergic receptor	3
Histamine receptor	4	Serotonin synthesis	1
Histone deacetylases	1	Serotonin 1A receptor	5
Hypoxia	1	Serotonin 1B receptor	1
Metabotropic glutamine receptor type 1	2	Serotonin 2A receptor	4
Metabotropic glutamine receptor type 5	1	Serotonin 4 receptor	1
Mitochondrial complex 1	1	Serotonin 6 receptor	1
Monoacylglycerol lipase	1	Serotonin transporter	6
Monoamine Oxidase A	1	Synaptic vesicle protein 2A	1
Monoamine Oxidase B	2	Translocator protein	13
Muscarinic acetylcholine receptor	2	σ1 receptor	1

regional kinetic parameters from healthy subjects have been reported in publications for 25 PET tracers. Eight additional PET tracers were identified and provided by the National Institute for Quantum Science and Technology, Japan.

The registered names of the PET tracers were adopted from the nomenclature used in the publications in which their kinetic parameters were reported. For cases in which the publications provided abbreviated names for the PET tracers, these shorter names were used for their registration.

Overview of the designed database

Our comprehensive database includes the regional kinetic parameters of healthy subjects, such as K parameters, V_T, and BP_{ND} [9], as well as detailed information on the compounds used in each existing CNS–PET tracer. As described above, the kinetic parameters of 120 PET tracers were meticulously extracted and subjected to thorough validation.

We categorized 15 distinct brain regions, including the temporal lobe, hippocampus, amygdala, cerebellum, brain stem (midbrain, pons), insula, cingulate gyrus, frontal lobe, occipital lobe, parietal lobe, caudate nucleus, putamen, thalamus, and pallidum, for the analysis. The classification strategy was based on PNEURO, which is a part of the PMOD software (PMOD Technologies LLC, Switzerland) originally derived from the Hammersmith atlas [12]. When kinetic parameters of sub-regions were reported in the published studies, averaged kinetic parameters of sub-regions were assigned as those of the corresponding region. Furthermore, if kinetic parameters of the global cortex and outside 15 brain regions (e.g., white matter) were reported, we included the data as those of "others".

Of the 120 PET tracers, information for 111 compounds was sourced from PubChem, where data for 9 compounds were calculated using ChemDraw version 22.2.0 (PerkinElmer, Inc., Massachusetts, USA). All collected data, encompassing the kinetic parameters and compound information, were stored in two different data formats: Microsoft Excel and JavaScript Object Notation (JSON).

Kinetic parameters of healthy subjects

For the 120 PET tracers, study information, including the number of subjects, sex, average age, and details regarding the kinetic analysis methods, were extracted from the respective publications. Kinetic analysis methods included compartmental or graphical analysis with arterial blood sampling, spectral analysis, and reference tissue analysis. In addition, the average values and their corresponding standard deviation for the kinetic parameters were obtained from these publications.

For most CNS–PET tracers, a compartmental analysis with arterial blood sampling was performed. Within this framework, the optimal model [e.g., one tissue compartment model (1TCM) or two tissue compartment model (2TCM)] determined for each publication was selected for inclusion in our database [13]. The kinetic parameters estimated for 2TCM included K_1 [mL/min/mL], k_2 [min^{-1}], k_3 [min^{-1}], and k_4 [min^{-1}], while for 1TCM, the parameters included K_1 [mL/min/mL] and k_2 [min^{-1}] [14]. In addition, macro parameters such as distribution volume (V_T), distribution volume ratio (DVR, against reference V_T) [15, 16], and BP_{ND} (calculated as k_3/k_4 for 2TCM) were derived from the K parameters of both 1TCM and 2TCM. V_T values were calculated as follows:

$$V_T(1TCM) = \frac{K_1}{k_2}, \quad V_T(2TCM) = \frac{K_1}{k_2} \cdot \left(1 + \frac{k_3}{k_4}\right) \tag{1}$$

Graphical analysis methods have been reported in the literature for specific CNS–PET tracers. For specific tracers, such as ^{18}F-MNI-444 [17], ^{11}C-DPA713 [18], ^{18}F-FCWAY, and ^{18}F-MeFWAY[19], Logan graphical analysis [20] was employed for V_T estimation. Other tracers, such as ^{18}F-ASEM [21], ^{11}C-TASP457 [22], ^{11}C-GR103545 [23], ^{18}F-PF-05270430 [24] and ^{11}C-AFM [25], employ Ichise's MA1 [26] for V_T estimation. For ^{11}C-CUMI-101, V_T was estimated using likelihood estimation in graphical analysis (LEGA) [27]. For several other CNS–PET tracers, including ^{18}F-PR04MZ [28], ^{11}C-MK8278 [29], ^{11}C-LY2795050 [30], ^{18}F-MH.MZ [31] and ^{11}C-SB207145 [32], BP_{ND} was estimated using a simplified reference tissue model (SRTM) [33]. For ^{18}F-FEF [34], V_T estimation was performed using spectral analysis [35].

The data format of the database

The structure of related text data in PET–BIDS [9] is based on the JSON format, which is known for its compact size, text-based nature, and compatibility with a wide range of programming languages beyond JavaScript. Consequently, the JSON format was selected for this study. However, JSON format is difficult for users to understand visually. Therefore, we have also created the database in Excel format.

In JSON format, data for each PET tracer were saved in a file bearing the name of the respective PET tracer, 'labeled RI'_'compound name' with the extension '.json,' and organized into folders based on their targets (Fig. 1). For the Excel format, data for each PET tracer were saved in a file bearing the name of the respective PET tracer, 'labeled RI'_'compound name' with the extension '. xlsx'.

Results

A total of 120 PET tracers were registered and distributed across various imaging targets shown in Table 1 and Supplemental Table 1.

Table 2 shows the kinetic parameters of [^{11}C]Martinostat, estimated using 2TCM [36]. Wey et al. reported detailed kinetic values for 27 regions in the supplementary data. To align these data with our 15 regions of interest, the kinetic parameters of the anterior, middle, and posterior cingulate were averaged to represent those of the cingulate gyrus. Similarly, kinetic parameters of the precentral gyrus, supplementary motor area, superior frontal cortex, medial frontal cortex, and inferior frontal cortex were averaged to represent those of the frontal lobe. In addition, the kinetic parameters of the calcarine, cuneus, lingual, and occipital cortices were averaged to represent those in the occipital lobe. The kinetic parameters of the angular cortex, postcentral gyrus, supramarginal gyrus, and precuneus were averaged to represent those of the parietal lobe. Regions where kinetic parameters from multiple regions were averaged are indicated by asterisks (*) in Table 2. Averaging kinetic parameters among detailed anatomical regions or surrounding regions was conducted for a total of 52 PET tracers; this information is provided in Supplemental Table 2. In addition, all kinetic parameters are accessible on GitHub (https://github.com/Database-of-CNS-PET-Kinetic-parameters/DOCK-PET).

Discussion

Overview of this study

Pharmacokinetics of PET tracers play a pivotal role in diagnostic PET imaging, and numerous PET tracers have been developed over the years. Therefore, this study aimed to construct an open-access, comprehensive database of kinetic parameters in healthy human brains. Our database encompasses regional kinetic parameters (K parameters, V_T, and BP_{ND}) and detailed information on the compounds, including their structures, chemical and physical properties, and affinities for each existing CNS–PET tracer. All

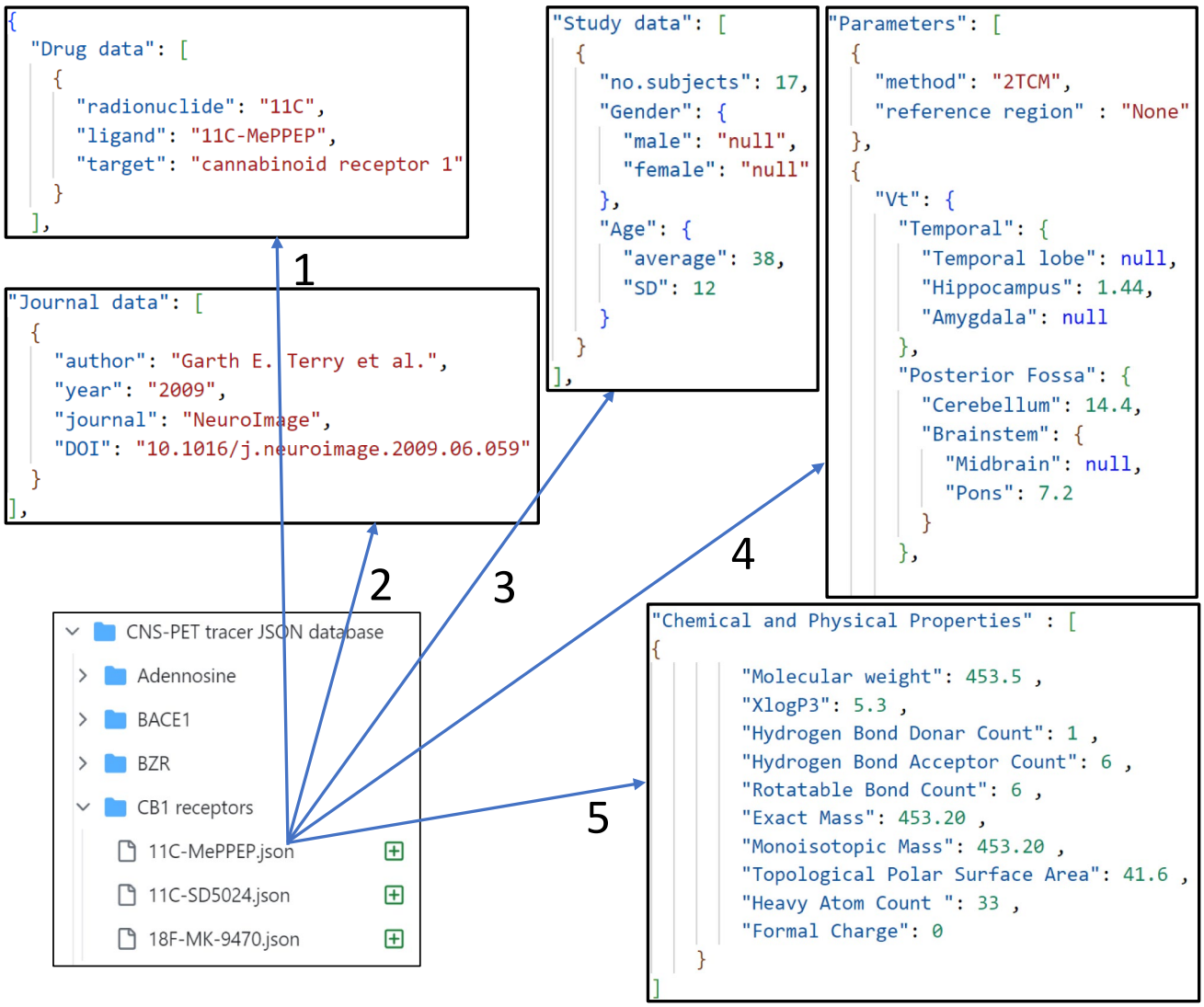

Fig. 1 Data expression of kinetic parameter information in JSON format

the data have been stored in Microsoft Excel and JSON. Furthermore, to enhance accessibility, all kinetic parameters are available on GitHub at https://github.com/Database-of-CNS-PET-Kinetic-parameters/DOCK-PET.

In this DOCK–PET, we selected the healthy subject group only. For most PET tracers, quantitative methods have been validated and established using the data obtained from young healthy volunteers, who were expected homogeneous subjects. Then, the values and deviations of the kinetic parameters can serve as the fundamental information of the PET tracer. Therefore, this study limited data obtained from healthy subjects.

Prospect of the DOCK–PET

There are two prospects for the DOCK–PET. One is using the database for machine learning to predict kinetic parameters. There has been growing interest in machine learning methods for tracer kinetic modeling [37]. Prediction methods of arterial input functions, kinetic modeling parameters, and model selection has been investigated in both clinical and preclinical studies. DOCK–PET may contribute to training the model to predict kinetic parameters of PET tracers not for specific single imaging target but for cross-imaging targets. The other is the catalog of pharmacokinetics. This

Table 2 Example of registered kinetic parameters of [^{11}C]Martinostat estimated by 2TCM

	K_1	k_2	k_3	k_4
Temporal lobe	0.24 ± 0.05	0.24 ± 0.07	0.27 ± 0.07	0.021 ± 0.007
Hippocampus	0.23 ± 0.04	0.32 ± 0.06	0.23 ± 0.06	0.016 ± 0.006
Amygdala	0.26 ± 0.04	0.49 ± 0.17	0.26 ± 0.08	0.014 ± 0.005
Cerebellum	0.34 ± 0.06	0.34 ± 0.17	0.24 ± 0.09	0.018 ± 0.008
Brain stem				
Midbrain	N/A	N/A	N/A	N/A
Pons	N/A	N/A	N/A	N/A
Insula	0.25 ± 0.04	0.21 ± 0.10	0.24 ± 0.09	0.023 ± 0.009
Cingulate gyrus	0.26*	0.30*	0.26*	0.019*
Frontal lobe	0.24*	0.19*	0.23*	0.024*
Occipital lobe	0.31*	0.33*	0.28*	0.022*
Parietal lobe	0.25*	0.24*	0.25*	0.022*
Caudate nucleus	0.18 ± 0.04	0.15 ± 0.03	0.20 ± 0.05	0.023 ± 0.008
Putamen	0.27 ± 0.05	0.20 ± 0.07	0.25 ± 0.09	0.024 ± 0.007
Thalamus	0.28 ± 0.06	0.28 ± 0.08	0.25 ± 0.06	0.021 ± 0.007
Pallidum	0..26 ± 0.04	0.23 ± 0.12	0.25 ± 0.11	0.022 ± 0.005

*The average value of kinetic parameters over detailed anatomical regions. N/A indicates not available

database serves as a valuable catalog of PET tracers used in clinical studies. As an illustrative case, the database enables the comparison of PET tracers for specific imaging targets, facilitating valuable insights and research in the field. We have not found any similar publications or databases. Therefore, we believe in the novelty and usefulness of the DOCK–PET compared to the surveys for published reports [10].

Limitations of this study

A significant limitation of our study is the need for the harmonization of PET protocols in terms of variations in scanners, scanning times, injection doses, image reconstruction methods, and other aspects. In addition, detailed parameters for kinetic analysis methods, such as cost functions, iteration times, weighting factors for residuals, and definitions of Regions of Interest (ROIs), must be standardized. In this study, the reported kinetic parameters were recorded without harmonization. However, future harmonization efforts are crucial to standardize kinetic parameter databases.

One of the limitations of this study was the relatively small number of CNS–PET tracers included in the database. Conventional databases, such as OpenNeuro, typically comprise a more extensive dataset, often exceeding hundreds or thousands. This limitation can be addressed by continuously adding registrations for future PET tracers and expanding the database.

A specific consideration in our research regarding PET kinetic parameters pertained to regional assignment. This regional assignment approach required sub-region averaging to compile the kinetic parameters for all regions, as shown in Table 2 and Supplemental Table 2. Sub-region averaging in the regional assignment approach did not consider the volume inequality of the sub-regions. This is also the limitation of our study.

Another significant limitation pertains to the target organs. In this study, because of the sufficient number of publications on the pharmacokinetics of PET tracers, the target organ was limited to the brain. The collection of datasets for the pharmacokinetics of PET tracers can be challenging in areas outside neurology, such as cardiology and oncology.

Conclusion

A novel database DOCK–PET containing kinetic parameters of existing CNS–PET tracers in healthy human brains was constructed. The data summarizing the results of this study are openly available on GitHub at https://github.com/Database-of-CNS-PET-Kinetic-parameters/DOCK-PET.

Supplementary Information The online version contains supplementary material available at https://doi.org/10.1007/s12149-024-01947-z.

Acknowledgements This study was partly supported by the Naito Foundation, Japan (MS) research grant.

References

1. Phelps ME, Hoffman EJ, Mullani NA, Ter-Pogossian MM. Application of annihilation coincidence detection to transaxial reconstruction tomography. J Nucl Med. 1975;16(3):210–24.
2. Ter-Pogossian MM, Phelps ME, Hoffman EJ, Mullani NA. A positron-emission transaxial tomograph for nuclear imaging (PETT). Radiology. 1975;114(1):89–98.
3. Ietswaart R, Arat S, Chen AX, Farahmand S, Kim B, DuMouchel W, et al. Machine learning guided association of adverse drug reactions with in vitro target-based pharmacology. EBioMedicine. 2020;57: 102837.
4. Kundu I, Paul G, Banerjee R. A machine learning approach towards the prediction of protein-ligand binding affinity based on fundamental molecular properties. RSC Adv. 2018;8(22):12127–37.
5. Dang NL, Matlock MK, Hughes TB, Swamidass SJ. The metabolic rainbow: deep learning phase I metabolism in five colors. J Chem Inf Model. 2020;60(3):1146–64.
6. Suhara T, Chaki S, Kimura H, Furusawa M, Matsumoto M, Ogura H, et al. Strategies for utilizing neuroimaging biomarkers in CNS drug discovery and development: CINP/JSNP working group report. Int J Neuropsychopharmacol. 2017;20(4):285–94.
7. Rahman M, Watabe H. Online molecular image repository and analysis system: a multicenter collaborative open-source infrastructure for molecular imaging research and application. Comput Biol Med. 2018;1(96):233–40.

8. Gorgolewski KJ, Auer T, Calhoun VD, Craddock RC, Das S, Duff EP, et al. The brain imaging data structure, a format for organizing and describing outputs of neuroimaging experiments. Sci Data. 2016;21(3): 160044.
9. Norgaard M, Matheson GJ, Hansen HD, Thomas A, Searle G, Rizzo G, et al. PET-BIDS, an extension to the brain imaging data structure for positron emission tomography. Sci Data. 2022;9(1):65.
10. McCluskey SP, Plisson C, Rabiner EA, Howes O. Advances in CNS PET: the state-of-the-art for new imaging targets for pathophysiology and drug development. Eur J Nucl Med Mol Imaging. 2020;47(2):451–89.
11. Guo Q, Brady M, Gunn RN. A biomathematical modeling approach to central nervous system radioligand discovery and development. J Nucl Med. 2009;50(10):1715–23.
12. Hammers A, Allom R, Koepp MJ, Free SL, Myers R, Lemieux L, et al. Three-dimensional maximum probability atlas of the human brain, with particular reference to the temporal lobe. Hum Brain Mapp. 2003;19(4):224–47.
13. Watabe H, Ikoma Y, Kimura Y, Naganawa M, Shidahara M. PET kinetic analysis–compartmental model. Ann Nucl Med. 2006;20(9):583–8.
14. Innis RB, Cunningham VJ, Delforge J, Fujita M, Gjedde A, Gunn RN, et al. Consensus nomenclature for in vivo imaging of reversibly binding radioligands. J Cereb Blood Flow Metab. 2007;27(9):1533–9.
15. Kudo Y, Okamura N, Furumoto S, Tashiro M, Furukawa K, Maruyama M, et al. 2-(2-[2-Dimethylaminothiazol-5-yl]ethenyl)-6- (2-[fluoro]ethoxy)benzoxazole: a novel PET agent for in vivo detection of dense amyloid plaques in Alzheimer's disease patients. J Nucl Med. 2007;48(4):553–61.
16. Ito H, Shinotoh H, Shimada H, Miyoshi M, Yanai K, Okamura N, et al. Imaging of amyloid deposition in human brain using positron emission tomography and [18F]FACT: comparison with [11C]PIB. Eur J Nucl Med Mol Imaging. 2014;41(4):745–54.
17. Barret O, Hannestad J, Vala C, Alagille D, Tavares A, Laruelle M, et al. Characterization in humans of 18F-MNI-444, a PET radiotracer for brain adenosine 2A receptors. J Nucl Med. 2015;56(4):586–91.
18. Akerele MI, Zein SA, Pandya S, Nikolopoulou A, Gauthier SA, Raj A, et al. Population-based input function for TSPO quantification and kinetic modeling with [(11)C]-DPA-713. EJNMMI Phys. 2021;8(1):39.
19. Choi JY, Lyoo CH, Kim JS, Kim KM, Kang JH, Choi SH, et al. 18F-Mefway PET imaging of serotonin 1A receptors in humans: a comparison with 18F-FCWAY. PLoS ONE. 2015;10(4): e0121342.
20. Logan J, Fowler JS, Volkow ND, Wolf AP, Dewey SL, Schlyer DJ, et al. Graphical analysis of reversible radioligand binding from time-activity measurements applied to [N-11C-methyl]-(-)-cocaine PET studies in human subjects. J Cereb Blood Flow Metab. 1990;10(5):740–7.
21. Hillmer AT, Li S, Zheng MQ, Scheunemann M, Lin SF, Nabulsi N, et al. PET imaging of alpha(7) nicotinic acetylcholine receptors: a comparative study of [(18)F]ASEM and [(18)F]DBT-10 in nonhuman primates, and further evaluation of [(18)F]ASEM in humans. Eur J Nucl Med Mol Imaging. 2017;44(6):1042–50.
22. Kimura Y, Takahata K, Shimazaki T, Kitamura S, Seki C, Ikoma Y, et al. Pharmacokinetic and pharmacodynamic assessment of histamine H(3) receptor occupancy by enerisant: a human PET study with a novel H(3) binding ligand, [(11)C]TASP457. Eur J Nucl Med Mol Imaging. 2022;49(4):1127–35.
23. Naganawa M, Jacobsen LK, Zheng MQ, Lin SF, Banerjee A, Byon W, et al. Evaluation of the agonist PET radioligand [(1)(1) C]GR103545 to image kappa opioid receptor in humans: kinetic model selection, test-retest reproducibility and receptor occupancy by the antagonist PF-04455242. Neuroimage. 2014;1(99):69–79.
24. Naganawa M, Waterhouse RN, Nabulsi N, Lin SF, Labaree D, Ropchan J, et al. First-in-human assessment of the novel PDE2A PET radiotracer 18F-PF-05270430. J Nucl Med. 2016;57(9):1388–95.
25. Naganawa M, Nabulsi N, Planeta B, Gallezot JD, Lin SF, Najafzadeh S, et al. Tracer kinetic modeling of [(11)C]AFM, a new PET imaging agent for the serotonin transporter. J Cereb Blood Flow Metab. 2013;33(12):1886–96.
26. Ichise M, Toyama H, Innis RB, Carson RE. Strategies to improve neuroreceptor parameter estimation by linear regression analysis. J Cereb Blood Flow Metab. 2002;22(10):1271–81.
27. Parsey RV, Ogden RT, Mann JJ. Determination of volume of distribution using likelihood estimation in graphical analysis: elimination of estimation bias. J Cereb Blood Flow Metab. 2003;23(12):1471–8.
28. Kramer V, Juri C, Riss PJ, Pruzzo R, Soza-Ried C, Flores J, et al. Pharmacokinetic evaluation of [(18)F]PR04.MZ for PET/CT imaging and quantification of dopamine transporters in the human brain. Eur J Nucl Med Mol Imaging. 2020;47(8):1927–37.
29. Van Laere KJ, Sanabria-Bohorquez SM, Mozley DP, Burns DH, Hamill TG, Van Hecken A, et al. (11)C-MK-8278 PET as a tool for pharmacodynamic brain occupancy of histamine 3 receptor inverse agonists. J Nucl Med. 2014;55(1):65–72.
30. Naganawa M, Zheng MQ, Nabulsi N, Tomasi G, Henry S, Lin SF, et al. Kinetic modeling of (11)C-LY2795050, a novel antagonist radiotracer for PET imaging of the kappa opioid receptor in humans. J Cereb Blood Flow Metab. 2014;34(11):1818–25.
31. Kramer V, Dyssegaard A, Flores J, Soza-Ried C, Rosch F, Knudsen GM, et al. Characterization of the serotonin 2A receptor selective PET tracer (R)-[(18)F]MH.MZ in the human brain. Eur J Nucl Med Mol Imaging. 2020;47(2):355–65.
32. Marner L, Gillings N, Comley RA, Baare WF, Rabiner EA, Wilson AA, et al. Kinetic modeling of 11C-SB207145 binding to 5-HT4 receptors in the human brain in vivo. J Nucl Med. 2009;50(6):900–8.
33. Lammertsma AA, Hume SP. Simplified reference tissue model for PET receptor studies. Neuroimage. 1996;4(3 Pt 1):153–8.
34. Grunder G, Siessmeier T, Lange-Asschenfeldt C, Vernaleken I, Buchholz HG, Stoeter P, et al. [18F]Fluoroethylflumazenil: a novel tracer for PET imaging of human benzodiazepine receptors. Eur J Nucl Med. 2001;28(10):1463–70.
35. Cunningham VJ, Jones T. Spectral analysis of dynamic PET studies. J Cereb Blood Flow Metab. 1993;13(1):15–23.
36. Wey HY, Gilbert TM, Zurcher NR, She A, Bhanot A, Taillon BD, et al. Insights into neuroepigenetics through human histone deacetylase PET imaging. Sci Transl Med. 2016;8(351):351ra106.
37. Miederer I, Shi K, Wendler T. Machine learning methods for tracer kinetic modelling. Nuklearmedizin. 2023;62(6):370–8.